

# Meta-Heuristic Based Melanoma Skin Disease Detection and Classification Using Wolf Antlion Neural Network (WALNN) Model

R. Rajeswari<sup>1</sup>, K. Kalaiselvi<sup>2</sup>, N. Jayashri<sup>3</sup>, P. Lakshmi<sup>4</sup>, A. Muthusamy<sup>5</sup>

Submitted: 20/10/2023

Revised: 05/12/2023

Accepted: 17/12/2023

**Abstract:** Skin cancer is among the most prevalent cancers in people. Most diagnoses are made visually, with clinical screening, histological investigation, biopsy and optional dermoscopic steps. Melanoma identification in the skin has been described as problematic due to the possible issues resulting from inadequate feature selection and the importance of achieving high levels of detection accuracy. To classify the malignant or average level of skin melanoma from MRI images, the optimal Wolf AntLion Neural Network (WALNN) model as a meta-heuristic-based deep learning (DL) approach is used in this paper. Correspondingly, the novel hybrid algorithm, namely Wolf Pack Search and AntLion Optimization Algorithm Optimization, is developed for optimal feature selection to ensure the performance of the Convolutional Neural Network learning classifier. The proposed approach, WALNN, is evaluated with existing techniques such as Decision Tree (DT), Cuckoo Search and Support Vector Machine (CS-SVM), and Convolution Neural Network (CNN) using the ISIC archive skin lesion dataset. As a result, the proposed methodology is carried out with a better outcome in term of sensitivity, specificity, Precision, Recall, and Accuracy and perform the recognition precisely.

**Keywords:** Optimization, Feature Selection, Skin Melanoma, Deep Learning, Classifier

## 1. Introduction

It is generally agreed that the human skin, the body's biggest organ, is susceptible to harm from factors including sunshine, a bad diet, drinking too much alcohol, and smoking [1]. Another category of aggravators that might emerge externally is illnesses and diseases. According to projections, skin cancer will surpass COVID-19 as the second biggest cause of mortality globally by 2020 due to its rapid and unrelenting development and the fact that it cannot be cured due to the disease's indiscriminate cell divisions [2]. According to estimates from the World Health Organization, 9500 people in the US have skin cancer diagnoses frequently, and two people pass away from the condition. They affect both sexes equally, regardless of age or nationality. Skin cancers include the nearly incurable melanoma and the more treatable but harder-to-detect squamous and basal cell carcinoma [3].

Studies that create strategies for utilizing imaging technologies to identify the effects of various skin disorders are urgently needed. Imaging technology has substantially contributed to developing processing hardware and software to lessen the challenge. The initial Classification of a skin picture is based on the proliferation

of melanocytes in the epidermis and dermis. The see-through nature of the tiny Images result from their low resolution [4]. Dermoscopy, a fresh imaging technique, enhances analytical Precision and this could potentially reduce the number of fatalities among people. High-resolution images taken during dermoscopic Imaging show the skin's underlying structure. Dermatology specialists visually images. This is a time-consuming procedure that necessitates accuracy and expertise [5]. The Computer-Aided Diagnosis system, for instance, uses a dermoscopic imaging modality to diagnose skin cancer [6]. Computer-aided diagnostics (CAD) technologies, which also save time and increase diagnostic accuracy, replace the need for such time-consuming and inaccurate manual processes. Traditional CAD systems have a relatively unimpressive track record because interlocking procedures limit the overall classification accuracy, including preprocessing, manual Extraction of features, and recognition. Before continuing to the next stage in these methods, bubbles and artefacts must first be removed. Besides, DL methods are much more efficient than either of these substitutes or human inspection. Convolutional neural networks (CNNs) [7] accurately extract features.

Doctors frequently struggle to categorize the severity of the condition and determine the type of illness when assessing a skin problem. As a result, it is more challenging to recommend medication. This issue might be resolved using deep learning algorithms to analyze microscopic images. These findings suggest that deep learning-based algorithms may be practical for quickly identifying clinical data and producing outcomes [8]. This study aims to describe the benefits of machine learning (ML) over DL for identifying and recognizing skin illnesses and suggest an improved approach that might favour human health if used in this field. High-performing algorithms are required to identify skin disease early with computer technology to obtain better accuracy, necessitated by improvements in computing hardware and image processing techniques [9]. Automatic skin lesion identification is difficult due to the range of input image photographs or the allowable surface variation in this skin.

The research paper is structured as described below: An introduction is made in the first part (I). They examine the existing research in the part after this (II) to identify the most effective strategies currently in use. The third segment examines deep learning to better grasp the teaching approaches' context. Then, go into great detail on the methods suggested in chapter 4.

<sup>1</sup>Associate Professor, Department of Computer Science, Dr MGR Educational and Research Institute, Chennai.  
Email: rajeswari.cse@drmgrdu.ac.in

<sup>2</sup>Associate Professor, Department of Computer Applications, Saveetha College of Liberal Arts and Sciences, Saveetha Institute of Medical and Technical Sciences, Chennai.

Email: mskalaiselvi@gmail.com, kalaiselvik.sclas@saveetha.com

<sup>3</sup>Associate Professor, Faculty of Computer Applications, Dr. M.G.R Educational and Research Institute, Chennai.

Email: jayashrichandrasekar@yahoo.co.in, jayashri.mca@drmgrdu.ac.in

<sup>4</sup>Assistant Professor in Computer Science, SRM Institute of Science and Technology, Tiruchirappalli Campus  
Email: lakshmi4@srmist.edu.in, laksomu1822002@gmail.com

<sup>5</sup>Assistant Professor, Department of Computer Technology, Kongu Engineering College, Perundurai, Erode - 638060  
Email: muthusamy.arumugam@gmail.com

The outcomes can interpret the ending inside the previous parts and presents a summary and recommendations for additional studies.

## 1.1 Problem Statement

The most severe type of abnormal skin tissue is malignant melanoma. Treatment includes chemotherapy and radiation therapy, and cancer gets harder to control in its later, more metastatic stages. Most of the time, diagonalization lacks the essential skills to identify skin cancer by examining a patient's skin to establish whether or not they are abnormal. Dermatologists are typically overburdened with patients, even though referrals from nearby general practitioners will enhance the detection rate for skin cancer by over 75%. Therefore, finding these disorders early on is essential for halting their spread. Most skin disease diagnoses are made visually, starting with a clinical screening and occasionally moving on to an MRI analysis. Due to the intricacy of determining the structure of skin defects, identifying cancer, and identifying inadequate features, melanoma disease can be challenging to diagnose.

## 2.1 Contribution of Work

Should become able to promote overall effectiveness that current diagnostic devices, that research suggests several unique feature selection and reorganization strategies. This approach aims to identify melanoma in its earliest stages. This work's algorithm for diagnosing skin cancer combines hybrid feature selection-based classification algorithms.

Accordingly, a combination of the Wolf Pack Search and AntLion Optimization methods is used to identify the best features.

A convolutional neural network can identify the ideal features for differentiating between benign and malignant skin tumours.

## 2. Related Work

Melbin suggested an effective method for identifying skin diseases, K. et al. (2019) [10], used an improved deep neural network model. Utilizing an upgraded level set approach-based segmentation method, database images are divided into groups. For each photo, feature extraction is done using GLCM. Every extracted feature must be recovered. Optimization-based dragonfly's artificial learning connection was used for categorizing skin disorders. The suggested dragonfly-based DNN was tested using established techniques like Support Vector Machine and Artificial Neural Networks for various evaluation metrics to illustrate the effectiveness of the approaches on the MATLAB platform.

Verma et al. (2020) [11] used three feature extraction strategies to discover the best data subset of Erythmato-Squamous Diseases (ESD) disease. The success of such a conceptual scheme was evaluated using the 4-classification methods Decision Tree, SVM, Random Forest and Gaussian Naive Bayesian. The model's prediction performance was then improved by using the stacking ensemble approach. In the correlation matrix, the feature selection techniques involve using a heat map, achieving the most excellent accuracy of 99.86%. We collect the Dataset with high accuracy in skin disease, and we suggest that the optimal feature selection methods are the correlation coefficient and heat map.

A deep CNN-based lesion classification method using saliency segmentation was suggested by Khan, M. Attique, et al. in 2020 [12]. The proposed Gaussian approach was used to increase the lesion contrast, and then RGB to HSV colour space conversion was used. The features are collected through the segmented images using the Inception Convolutional Neural Network design across 2 fundamental output layers. Three datasets, including PH2, ISBI 2016, and ISBI 2017, are used to show the effectiveness of the suggested methodologies. These datasets reach an accuracy of 97.74%, 96.1%, and 97%, respectively. According to simulation findings, the presented technique outperforms existing methods on all three datasets. Additionally, using the most discriminant information reduces calculation time and increases classification accuracy.

Srinivasu, Parvathaneni Naga, and others (2021) [13] employed MobileNet V2 and Long Short-Term Memory to classify skin diseases using DL. This model's efficacy has been compared to that of CNN, Visual Geometry Group intense convolutional networks for large-scale image recognition, and fine-tuned neural networks (FTNN). The FTNN technique outperformed existing methods by more than 85%. Even though there is plenty of data, the researchers advise conducting further studies to explore the feature extraction processes based on biomarkers that can show alerts and enable safe data transmission between patients and doctors in eHealth and telehealth environments.

Goceri & Evgin et al. (2021) [14] suggested that a novel model be built utilizing MobileNet. Additionally, a brand-new loss function has been created and applied. The three primary accomplishments of this work are presenting a modified-MobileNet architecture, (ii) proposing a unique hybrid loss function, and (iii) developing and integrating a communication application using a user-friendly interface with modified-MobileNet. The outcome showed that the suggested method accurately detects skin conditions in 94% of cases.

A method for spotting and identifying tumour skin images obtained from a standard medical dataset was reported by Xiong, Xin, et al. in 2021 [15]. The suggested approach, which starts with noise reduction, prepares the picture for Segmentation and retrieves essential features to help the classifier recognize the tumour following these features. This study produced a high recognition rate and accuracy, and to further its credibility, a comparison with manual methods that devoted systematic effort to correctness was made. Discovering new features for future research and training on diverse datasets can help improve the image for more illuminating data.

In Khan, Muhammad Attique, et al. (2021) [16], a completely automated approach for classifying skin lesions into many categories was suggested. The approach for feature optimization utilizing the improved moth flame optimization algorithm in the CNN-based saliency segmentation approach was also detailed in the framework. Pre-trained deep learning models cannot achieve good segmentation accuracy using segmented lesions. This issue was solved by removing unnecessary and excess deep features utilizing the IMFO method, which increased accuracy. The computing time, however, is one of the limitations of inaccurate feature selection to trained on unrelated image data.

The fluorescence-aided amplifying network (FAA-Net) was built by Lee, Kyungsu, et al. (2022) [17] to identify skin illnesses that provide Red Green Blue (RGB) and fluorescence images. It is supplied with a meta-learning method to address issues arising from the created system's insufficient number of images captured. To assess FAA-effectiveness Net and compare various assessment metrics between our generated model and other cutting-edge models for the detection of skin illnesses utilizing the suggested approach, researchers performed a clinical experiment in a hospital. According to experimental data, it outperformed more sophisticated models in terms of accuracy and AUC in identifying skin illnesses by 8.61% and 9.83%, respectively.

DLCAL-SLDC, the Layer-based CAD simulation for one minor infection with concentration identification, including categorization, was developed by Adla, Devakishan, et al. in 2022 [18]. The model's objective is to use dermoscopic pictures to identify and categorize various forms of skin cancer. The CAL layer, integrated into CapsNet, aims to make a real connection with the CapsNet for further processing by capturing the discriminative class-specific characteristics and covering class dependencies. The Swallow Swarm Optimization algorithm-based Convolutional Sparse Autoencoder performs the classification step last. An ISIC dataset is used as a benchmark to validate the proposed DLCAL-SLDC method. Concerning several metrics, the suggested framework outperformed existing techniques with 94% sensitivity, 98% accuracy, and 99% specificity.

In the past, many automated methods for diagnosing skin lesions have been proposed, but they have not yet been shown to be very accurate. Afza, Farhat, et al. (2022) [19] presented a hierarchical architecture and DL to promote accuracy. A modified

grasshopper technique further enhances the retrieved deep learning characteristics. The Nave Bayes classifier is used on three datasets to categorize skin lesions as benign, melanoma, etc. The accuracy of their approach is enhanced on the chosen datasets. They also noticed that the feature optimization procedure obtains more pertinent characteristics to increase classification accuracy further. This work's main flaw is improper Segmentation, which removes noisy and pointless information. They will deal with this problem in the future using an intense learning system. They will also evaluate the most recent Dataset, such as ISBI2018.

### 3. Proposed Methodology

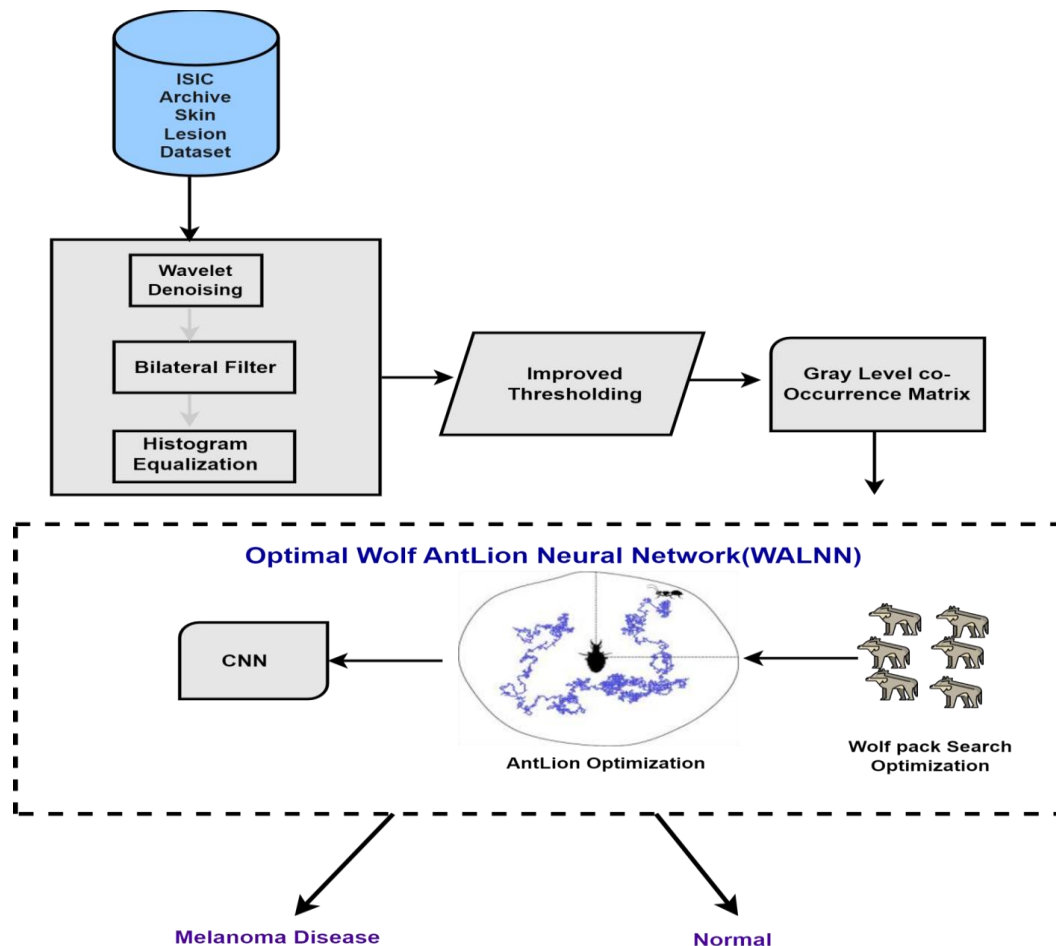


Fig. 1. Proposed Methodology

After that, an improved thresholding approach is applied to perform the Segmentation. Following that, to extract information from the image that has been provided, feature extraction is an essential step that must be taken. To analyze texture images, we use a Gray Level Co-occurrence Matrix. To determine the spatial dependency between image pixels, GLCM is utilized. The GLCM algorithm is applied to a grayscale picture matrix to determine the most prevalent characteristics, such as contrast, mean, energy, and homogeneity.

At last, the extracted images are given to an optimized classifier for Classification. As a result, the optimal features are selected, and the classify skin lesion cancer is using the optimal Wolf AntLion Neural Network (WALNN). Finally, the proposed method performance is analyzed through Evaluation metrics.

#### 3.1 Preprocessing

The quality of an image can be improved by using an image enhancement approach known as preprocessing. This technique enhances the quality of an image by eliminating undesired distortions and improving specific image attributes that can then

Skin lesion cancer detection using the image processing method is described as identifying and classifying the presence of tumour cells within an image. It has five processes: analysis, fragmentation, object recognition, or Optimization based Characterization using the Optimized Deep learning approach shown in Fig.1. The ISIC archive dataset [20] is used as input to classify Skin lesion cancer by the proposed method. Initially, the images are analyzed under preprocessing approach. It is suggested that the noise be removed, the edges enhanced, and the contrast increased by applying Wavelet denoising, Bilateral Filter, and Histogram Equalization.

be employed in subsequent processing steps. In the context of this study, the essential functions that will be implemented on the MRI pictures are those aimed at ensuring that the system can read the appropriate input and improving the conditions under which image analysis may take place [21]. The following is a list of the steps. The steps are as follows:

##### 3.1.1. Wavelet Denoising

Wavelet thresholding, also known as wavelet denoising [22], is based on the wavelet transform of various real-world signals and images. It is difficult to reconstruct a usable signal from raw Data when just a noisy representation is provided. The objective is to invert the transformation to obtain a copy of the images free of noise while taking advantage of the signal's local properties. When applied to a one-dimensional image, wavelet shrinkage denoising reduces noise without affecting the image. This is conducted regardless of the signal's scale composition. No attempts were made to improve the findings artificially. By eliminating the highest frequencies, smoothing preserves the lowest ones. Due to this flattening, 2D signals lose Precision and

information. Wavelet shrinkage denoising requires only a linear DWT, some nonlinear shrinkage denoising, and a linear inverse DWT. This heuristic approach is non-parametric, meaning its analysis is not guided by assumptions extracted from the data. In contrast to parametric systems, which require estimating unknown parameters inside a known model, this method uses a graphical representation of the data. Viral is a well-known parametric method that uses the least-squares technique.

### 3.1.2. Bilateral Filtering

The "bilateral filtering" technique aims to blur images while keeping their edges intact. Recent years have seen a sharp increase in bilateral filtering, which is now utilized in many image processing tasks like image denoising, picture enhancement, and related tasks. The bilateral filter's success can be attributed to the qualities described below.

- It is simple to come up with an adequate response. The technique replaces individual pixels with weighted averages of the pixels around them. It just needs two parameters to specify the size and contrast of the characteristics that should be preserved. The process does not entail any iterative steps either. As a result, it is simple to change the parameters because their impact does not grow stronger with time.

This filter can't eliminate salt and pepper noise, which has the disadvantage of spreading noise over medical photos. That is a significant flaw. Accessing the image's various frequency components is impossible since the bilateral filter only has one resolution. This limitation also applies to the bilateral filter. It does a respectable job at noise filtering in high-frequency regions but fails in low-frequency areas.

### 3.1.3. Histogram Equalization

The histogram of a picture can have its dynamic range increased by a process called histogram equalization. This is done by modifying the slope of the histogram. To create and play a picture with consistent dispersion to intensities, with convolution, this resulting picture is given the amplitudes of both the pixels contained in the input image. Histogram equalization creates a uniform histogram throughout, improving contrast [23]. This technique can modify a specific area of an image or the entire image.

The intensity of the distributions is redistributed when histograms are equalized. The main difference is that the peaks and valleys will be in various places even after equalization, even if the image's histogram contains many ups and downs. Along with consideration of all this, "spreading" rather than "flattening" seems to be an improved phrase for explaining the equalization of the histogram. All pixels are given an updated strength estimate depending on their previous strength during the histogram equalization process.

## 3.2 Segmentation

The histogram is typically used to establish the threshold for images that exhibit clear contrasts between the target's grey and background levels. The technology and the act of separating a specific target from a defined area are collectively called Segmentation [24]. There are many different approaches to segmenting an image by improved thresholding.

Hard and soft thresholding are the two most popular thresholding techniques in wavelet-based noise reduction. Wavelet components that are greater than will be reduced when using the gentle thresholding method and will remain unchanged when using the complex thresholding function. Otherwise, they will be reduced to zero. In contrast, wavelet components bigger than the complex thresholding function will be preserved; otherwise, they will be reduced to zero.

Due to its nonlinear and continuous behaviour, the application of this improved thresholding function has advantages over conventional complex and soft thresholding. The proposed better thresholding function is shown in Equation (1). This suggested function is data-dependent because it depends on the threshold value and wavelet coefficients.

$$h = na^{-\left(\frac{th}{n}\right)^2} \quad (1)$$

where  $n$  is wavelet coefficients and  $th$  is threshold value.

## 3.3 Feature Extraction

It was essential to extract the fundamental feature due to the complicated structure of the skin's differentiated tissues. A popular method for analyzing textures is the grey-level co-occurrence matrix, sometimes named the "grey-level co-occurrence matrix." Based on second-order statistics, it generates predictions about the properties of images. To recover the texture of a picture, the grey-level co-occurrence matrix [25] is utilized. The grayscale difference between two neighbouring pixels is calculated using this matrix. The grey level correlation matrix (GLCM) displays the distribution of the different shades of grey in an image. By creating descriptors from the matrix, the co-occurrence matrix of the ROI can be utilized to help classify the various skin tissues. By first creating a connection between two pixels—one of which will serve as some other pixels and the references pixel as a neighbouring pixel—the GLCM may be determined.

The quantity of rows or columns as a GLCM matrix is equivalent to this same amount of shades of grey in a photograph (Gr). A transform of vector ( $v$ ) input of variables  $A_i$  with size  $N$  (rows and columns of image) created in the  $n$ -dimensional space and  $i = 1 \dots n$  is given by,

$$A_i = [P_1, P_2, \dots, P_n]^T \quad (2)$$

To compute the covariance matrix, it is required to determine first the mean of a picture, which may be found using the Equation shown below.

$$T_m = \frac{1}{N} \sum_M^N X_i \quad (3)$$

We may determine the covariance of the original data using the Equation provided below, using the mean of the data.

$$X = A_i - T_m \quad (4)$$

One way to determine an image's co-occurrence matrix is to compute the frequency with a specific intensity concerning pixel  $j$  at distance and orientation  $d$ . When calculating the co-occurrence matrix of an image, the following features are taken into account. The contrast measures the degree to which different pixels differ in their grey level.

$$CON = \sum_i \sum_j (i - j)^2 \text{Pixel}(i, j) \quad (5)$$

The degree of elements in the GLCM and the diagonal GLCM is similar is what is meant by the term "homogeneity." When there is less contrast, there is more of a tendency toward homogeneity.

$$HOGE = \sum_i \sum_j \frac{P(i, j)}{1 + |i - j|} \quad (6)$$

The uniformity of the image is another factor that affects IDM.

$$IDM = \sum_i \sum_j \frac{1}{1 + (i - j)^2} P(i, j) \quad (7)$$

Entropy is a quantitative measurement of the information content of a system, and its relationship to energy is inverse. The entropy of a distribution that is predominately random is high. Low entropy is characteristic of distributions that are highly coupled or homogeneous.

$$ENTR = \sum_i \sum_j \text{Pixel}(i, j) \log_2 \text{Pixel}(i, j) \quad (8)$$

The energy is the mean of the squared value of pixel intensity.

$$ENRY = \sum_i \sum_j \text{Pixel}(i, j) \quad (9)$$

The term "correlation" refers to a measurement of the linear dependency of the grey level between the pixels located at the defined positions from one another.

$$COR = \sum_i \sum_j \frac{\{i\} * \text{Pixel}(i, j)}{\sigma_i * \sigma_j} \quad (10)$$

After that, the eigenvectors are determined using the provided Equation,

$$C = XX^T \quad (11)$$

## 3.4 Proposed Wolf Antlion Neural Network (WALNN) Model

A relatively recent swarm intelligence system called the wolf pack search algorithm (WPS) models wolf packs' hunting behaviour to address optimization issues. A collection of wolves might boost their chances of getting prey by cooperating in the wild. The wolf pack [26] then starts to pursue the herd of prey in the direction of the most pungent stench, which is when the arrest

action starts. They can split into multiple smaller groups when they move closer to the intended victim. Each subgroup will distinctly pursue the target, as described by the following:

$$W_{F_q}^{f+1} = W_{F_q}^f + \left( \frac{f_{max} - f}{f_{max}} \right) \left( \frac{W_{F_{best}} - W_{F_q}^f}{\sqrt{(W_{F_{best}})^2 + (W_{F_q}^f)^2}} \right) \\ = W_{F_q}^f + \Delta f \Delta W_{F_q}^f \quad (12)$$

where  $W_{F_{best}}$  best denotes the optimal search path,  $W_{F_q}^f$  denotes the search path,  $q$  denotes the population size,  $f$  denotes the number of running steps,  $f_{max}$  is the highest running step, and  $\Delta W_{F_q}^f$  denotes the change in the search path. Wolves are first let to move a great distance  $\Delta f$  around the search area while taking time-varying running steps. Each subgroup will coordinate its attack with those of the other wolf packs. After the continuous search, a modest step adjustment that reduces the walk  $\Delta f$  enables the wolves to pursue the quarry.

When a new solution in the WPS algorithm is better than the best, it might be stored as the best. The solution sequence is monotonic, decreasing as a result. Assuming constant for  $fias_t = 0$ , for the sake of this study, modifying parameters  $\delta$  ( $\delta = \delta_1 = \delta_2 = \dots = \delta_m$ ) and would improve the discrimination accuracy in a dynamic context. The MSEF is minimized by setting the optimal parameters, which are provided by

$$\delta_{tq}^{f+1} = \delta_{tq}^f + \Delta f \left( \frac{\delta_{best} - \delta_{tq}^f}{\sqrt{(\delta_{best})^2 + (\delta_{tq}^f)^2}} \right) \quad (13)$$

$$\theta_q^{f+1} = \theta_q^f + \Delta f \left( \frac{\theta_{best} - \theta_q^f}{\sqrt{(\theta_{best})^2 + (\theta_q^f)^2}} \right) \quad (14)$$

Two converging requirements must be met for the WPS method to be terminated: (a) the objective function MSEF must be smaller than a predetermined value  $\gamma$ , and (b) the number of running steps must reach the maximum number  $f_{max}$ . Thus, by decreasing the MSEF, the ideal parameters may be found.

Mirjalili recently invented the optimization technique known as Antlion Optimization (ALO). The ALO algorithm imitates a natural hunting strategy of the antlion. The two subsections go through the artificial sources of the algorithm of inspiration and its operators. Doodlebugs (antlions) are members of the Neuroptera order and Myrmeleontidae family. The adult stage is used for breeding, while they primarily hunt in larval stages. Thus larval stage of an antlion moves circularly while ejecting sand from its muscular mouth, forming a sand hole with the form of a cone. The larvae will first drill the hole for the trap's entrance, and then they will burrow into the cone's base and wait for their prey—most likely ants—to enter the opening.

The antlion seeks to capture its victim after discovering a prey in the trap. Insects attempt to escape the trap but typically are not charged right away. In this instance, antlions cleverly toss grains toward the hole's edge to help the prey slip towards the pit's bottom. A prey captured in the jaw is dragged under the ground and eaten. Antlions discard the remaining target outside the hole after eating it and prepare the hole for the subsequent hunt. The association between with creature's dimensions, this same intensity of longing, and the phase of rising moonlight is another action that has been seen in the way of the antlion's way of living and is both fascinating and puzzling.

A roulette wheel is employed to simulate an antlion's capacity for hunting. One antlion is said to be the only one with any ants imprisoned inside it. The ALO algorithm must use a roulette wheel operator to choose which ant to optimize based on their fitness level. The healthier antlions have a higher chance of catching ants due to this tactic. Their main prey is ants.

The antlion will consume the captured ant at this point in the hunt. It is thought that prey is taken when an ant becomes more physically fit than its counterpart antlion and enters the sand. It is believed that prey is caught because ants imitate this procedure. To increase its chances of successfully catching new prey, the antlion will modify its position to coincide with the location of the ant it has been pursuing most recently. Equation (15), shown below, is one possible resolution.

$$al_{g_x}^o = a_{l_k}^o \text{ If } (a_{l_k}^o) \text{ is better than } W(al_{g_m}^o) \quad (15)$$

Where  $o$  indicates the current iteration,  $al_{g_x}^o$  represents the position of chosen  $k$ -th antlion at  $o$ -th iteration, and  $a_{l_k}^o$  indicates the position of  $x$ -th ant at  $o$ -th iteration.

Once they detect an ant within the trap, antlions blast sands outward from the centre of the opening, trying to escape the trapped ant slides down. Due to its behaviour, the hyper-sphere of the ant's random walks radius is adaptively reduced when modelling this behaviour mathematically; see equations (16), (17), and (18).

$$R^o = \frac{R^o}{p_1} \quad (16)$$

$R^o$  is the low value of all variables at the iteration, and  $p_1$  is a ratio.

$$F^o = \frac{F^o}{p_1} \quad (17)$$

where  $F^o$  is the maximum among the variables at the  $o$ -th iteration and  $p_1$  is a ratio

$$p_1 = 10^{\tau \frac{o}{L}} \quad (18)$$

Where  $p_1$  is the current iteration,  $L$  is the maximum iteration, and  $\tau$  is a constant. In its most basic form, consistency can vary as much as someone is exploited Precision.

Thus slide ant is imprisoned in the selected burrow of antlion by simulating the sliding of prey towards it. In other words, the location of the chosen antlion serves as a boundary for the ant's walk, which may be described by adapting the ant's random walk's range to this location of the antlion as within problems (19) & (20).

$$R_x^o = R^o + al_{g_k}^o \quad (19)$$

$$F_x^o = F^o + al_{g_k}^o \quad (20)$$

Where  $R^o$  is as smallest among all factors  $o$ -th iteration,  $F^o$  indicates this matrix containing the highest value of each variable  $o$ -th iteration,  $F_x^o$  the minimum of all variables for  $x$ -th ant,  $F_x^o$  is its most significant factor for everyone  $x$ -th ant, and  $al_{g_m}^o$  Shows the location of the chosen  $k$ -th antlion at  $o$ -th iteration.

All random walks are built using this Equation (21).

$$Z_1(O) = [0, CSUM(2j(o_1) - 1); CSUM(2j(o_2) - 1); \dots; CSUM(2j(o_h) - 1)] \quad (21)$$

Where  $CSUM$  calculates the cumulative total, where  $h$  is far more repetitions possible,  $o$  is a random walk step, which in this study is referred to as an iteration, and  $j(o)$  is a stochastic function described by an equation (22).

$$j(o) = \begin{cases} 1 & \text{if } y \text{ and } > 0.5 \\ 0 & \text{if } y \text{ and } \leq 0.5 \end{cases} \quad (22)$$

where  $o$  is the following step in the random walk process and the rand is an unpredictable digit plus evenly distributed throughout its range [0, 1]. The Equation is used to normalize the random walks and maintain them within the search space. (9)

$$Z_{1x}^o = \frac{(Z_{1x}^o - o_x) \times (F_x - R_x^o)}{(D_x^o - o_x)} + R_x \quad (23)$$

Where  $O_i$  is just the lowest among the stroll of random  $o$ -th component,  $D_i$  would be the greatest among the quietly stroll through  $x$ -th variable,  $R_x^o$  is that least  $o$ -th variable at  $o$ -th iteration, and  $F_x^o$  indicates the maximum of  $x$ -th variable  $o$ -th generation.

It is necessary to employ authoritarianism to protect the top solutions over numerous variations. The elite and selected antlions in this scenario control the ant's random walk; therefore, a change in location for a particular ant assumes the shape of the two very different spontaneous approaches' averaged as eq.24 as below,

$$a_{l_x}^o = \frac{M^o C + M^o U}{2} \quad (24)$$

where  $M^O C$  is the randomly chosen road concerning about antlion that was selected due to its elite status, and  $M^O U$  is the randomly chosen way around the antlion determined through the top of the wheel. A trained classifier and an automated feature extractor make up a convolutional neural network. These multi-layered, hierarchical networks of neurons have the depth architecture for directed education that is learned via the back-propagation technique. Subsampling and convolution layers are combined and analyzed differently in CNN, which are used to learn complex high-dimensional data. Their architectural designs are different. Many CNN topologies are offered for various issues, including object identification and handwritten recognition.

On the challenge of pattern recognition, the best result was attained. Additionally, CNN combines three key hierarchical characteristics, Local receptive fields, spatial sub-sampling, and weight sharing, which provide scale, shift, and distortion features that are invariant to a certain extent. It has several layers in it. To begin with, the input is filtered using a series of layers to produce the feature map's values. Then, a sub-sampling layer was used to minimize the spatial resolution of the feature map's dimensionality. Layers of convolution the feature extractor is made up of different sub-sampling layers and is used to extract distinguishing characteristics from the original pictures. Two fully connected layers [27] of its outer part are as follows. Each layer uses the output of the preceding layer as its input.

CNN, a subset of multilayer feed-forward neural networks, are created with the express purpose of processing large-scale pictures or sensory input presented as multiple arrays while taking local and global stationary features into account.

Like an MLP, a convolutional neural network (CNN) is composed of several layers, with each output layer gradually connecting to the input of the layer before it using a set of trainable weights and biases. The multi-link protocol is another type of network. Every layer employs convolution to learn new

features from various perspectives, and each layer then expresses those learned characteristics as input and output feature maps. This is the primary distinction.

The CNN comprises convolution, nonlinearity, combining, and sub-sampling operations. In the CNN structure [28], the revolving and pooling layers are alternately layered until the high-level features are gathered. At this point, there is a wholly integrated categorization utilizing the high-level feature data. Convolutional network layers can contain several convolution layers and approximate values for the components for processing inside a single sharing on mapping. Thus described, the design of the product is displayed in Fig2.

This configuration allows the network to pick up new attributes when limiting how many variables there are; this region of interest produced  $Q_{p,q}^{(a)}$  Convolution layers l's calculation is as follows:

$$Q_{p,q}^a = \partial^{(a)} \left( \sum_{r=1}^k \sum_{s=1}^k Z_{r,s}^{(a)} \cdot M_{p+rq+s}^{(A-1)} + C^{(a)} \right) \quad (25)$$

Where  $M_{p+rq+s}^{(A-1)}$  signifies a structural location of that and their Levant map of features just at previous stratum a-1 and  $Z_{r,s}^{(a)}$  indicates the layer-based multilayer filtration has dimension  $k \times k$  a. That approach adds a bias unit  $C^{(a)}$  and uses the dot product ( $\cdot$ ) between them to pass utilizing a multilayer filtering over that whole convolutional feature import. The artificial neuron is complicated to further augment that nonlinearity  $\partial^{(a)}$  because the covering 'a' has been removed from the linear combination.

Thus pooling/subsampling layer can lower the computational complexity during training by generalizing the convolved features by down-sampling. This final product was  $H^{(d)}$  could be obtained using just the prior layer  $h^{(d-1)}$  by use of a pooling/subsampling layer d.

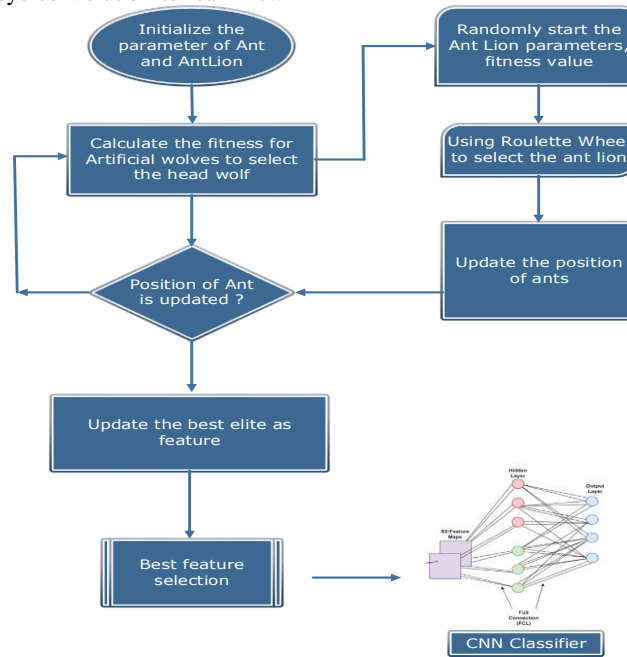


Fig. 2. Proposed WALNN approach Flowchart

$$\max(h_{1+v(p-1),1+v(q-1)}^{d-1}, \dots, h_{vp,1+v(q-1)}^{d-1}, \dots, h_{1+v(p-1),vq}^{d-1}, \dots, h_{vp,vq}^{d-1}) \quad (26)$$

Where  $v \times v$  denotes the size of the local spatial region,  $1 \leq p, q \leq (s-r+1)/v$ , indicates increasing method's strength, but  $m$  denotes how significant the inputs are feature map. Thus max merely uses the maximum value to summarize the input information within the immediate spatial region. By doing this, the learned characteristics acquire a certain degree of spatial and translation invariance, becoming resilient and abstract. After most advanced

functions have been isolated, these different layers are converted into vectors through one-dimensionality, and a wholly linked last layering is produced.

#### 4. Result and Discussion

The optimal Wolf AntLion Neural Network (WALNN) model was utilized in diagnosing skin disease. The results of this study have been implemented with the help of the computer language MATLAB 2020. The proposed system was evaluated using the evaluation metrics that were provided. The results of the Classification carried out by WALNN are shown here. To test

and assess the experimental findings of the recognition system, the following evaluative metrics were utilized: areas under the curve, responsiveness, and resolution Precision-Recall, With Mean Square Error Accuracy. The new method was used to diagnose the patient's skin cancer. In the following subsection, we offer a more in-depth description of the experiment results that were obtained using the suggested system through the following ISIC dataset

#### 4.1. ISIC Dataset

Two thousand seven hundred fifty dermoscopy images in total are included in this Dataset. 2000 were employed as

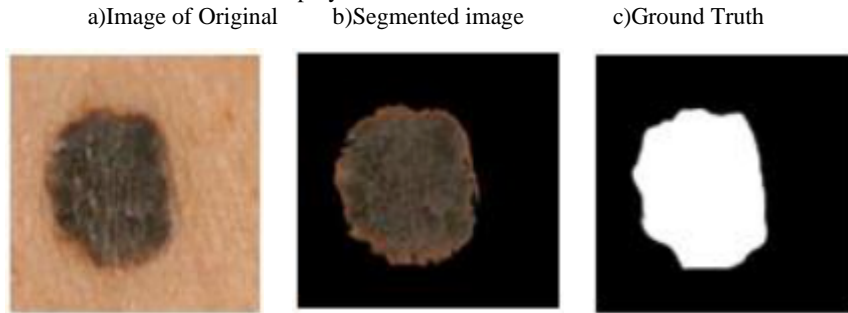


Fig.3. Segmented Analysis using Improved Threshold Approach

#### 4.3. Comparison of performance analysis

The proposed model Wolf AntLion Neural Network (WALNN) model and existing approaches such as DT, CS-SVM, and Convolution Neural Network (CNN) are evaluated.

##### Precision

The following formula is used to determine a precision score, which shows the percentage of productive results which genuinely precisely correct,

$$Precision = \frac{TP}{TP+FP} \quad (27)$$

##### Sensitivity

To analyze the classification performance, the confusion matrix is evaluated in terms of accuracy, awareness, & Precision.

$$Sen = \frac{TP}{TP+FN} \quad (28)$$

instruction,600 for development & 150 as confirmation. These real-world examples from each Data application to the general audience validate the segmentation technique. For the classification challenge, photos are divided into three groups: nevi, seborrheic keratosis, and melanoma, respectively, 1372, 254 and 374.

#### 4.2. Segmentation Analysis

After preprocessing is completed, the Improved Thresholding approach performs the Segmentation. According to Fig.3, the ground truth has accurately segmented and differentiated the borders from the skin impacted by cancer.

##### Recall

The recall is calculated when comparing tightly categorized images to the overall count of images associated with that class.

$$F1 = \frac{TP}{TP+FN} \quad (29)$$

##### Accuracy

That is measured as the percentage of suggestions that have been categorized.

$$Accuracy = \frac{TP+TN}{TP+TN+FP+FN} \quad (30)$$

Note that and represent true positive, true negative, false positive, and false negative, respectively. Thus the comparison to classification performance on that Dataset set using different evaluation indexes is shown in table.1.

Table 1. Comparison and performance analysis of the Proposed model

Methods	Specificity	Sensitivity	Precision	Recall	Accuracy
Decision Tree (DT)[29]	96.45	97.67	96.67	95.34	96.56%
Cuckoo Search and Support Vector Machine (CS-SVM) [30]	97.45	97.90	97.87	97.35	97.34%
Convolution Neural Network (CNN)[31]	98.12	98.93	98.32	97.01	98.76%
Wolf AntLion Neural Network (WALNN) model	98.34	99.12	98.98	97.45	99.01%

Accordingly, As a result, the specificity, sensitivity, Precision, Recall, and Accuracy of 98.34%, 99.12%, 98.98%, and 99.01%, respectively, for the proposed Wolf AntLion Neural Network

(WALNN) model. In addition, it has superior results compared to other existing approaches. The graphical representation in Fig.4,

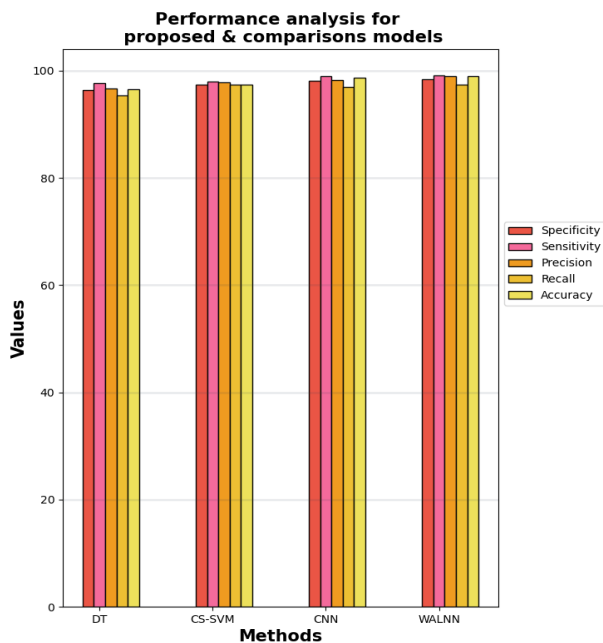


Fig. 4. Performance analysis of the proposed model

## 5. Conclusion

To detect and categorize skin disorders, the Meta-Heuristic Based Melanoma Skin Disease Detection and Classification Using Wolf Antlion Neural Network (WALNN) Model is utilized in this particular piece of research. Image preprocessing techniques like Segmentation and preprocessing can help reduce the number of variables that aren't important to the analysis. After that, every texturing attribute is extracted using the grey-level co-occurrence matrix, and the area pixel approach removes the lesion region's characteristics. These repeat the process till all the features have been extracted. Consequently, the novel hybrid method known as Wolf Pack Search and AntLion Optimization Algorithm Optimization has been developed for optimal feature selection. This algorithm was designed to ensure the performance of the Convolutional Neural Network learning classifier according to the features of the texture and the lesion area, thereby accomplishing an ideal level of accuracy in recognition. The development of automated methods that assist doctors in the early diagnosis of melanoma track the progression of the disease over time and have the potential to be used remotely represents an unrivalled opportunity to improve melanoma detection. Compared to other skin disease classification techniques, training a CNN effectively requires a large dataset that will be used in future. A variety of hybrid optimization techniques and classifiers will also be used to enhance the performance of melanoma skin diseases.

## References

- [1] Kostrzewska, Paulina, et al. "Sunscreens as a prevention of the photoaging." *Journal of Education, Health and Sport* 10.8 (2020): 11-16.
- [2] Lobdell Kevin, W., and A. Rose Geoffrey. "Improving health care leadership in the COVID-19 era." *NEJM Catalyst Innovations in Care Delivery* (2020).
- [3] Igari, Fumie, Hisashi Tanaka, and Armando E. Giuliano. "The Applications of Plasma Cell-free DNA in Cancer Detection: Implications in the Management of Breast Cancer Patients." *Critical Reviews in Oncology/Hematology* (2022): 103725.
- [4] Peck, Tabitha C., et al. "Effects of Transparency on Perceived Humanness: Implications for Rendering Skin Tones Using Optical See-Through Displays." *IEEE Transactions on Visualization and Computer Graphics* 28.5 (2022): 2179-2189.
- [5] Hameed, Ahmad, et al. "Skin lesion classification in dermoscopic images using stacked Convolutional Neural

- Network." *Journal of Ambient Intelligence and Humanized Computing* (2021): 1-15.
- [6] Adla, Devakishan, et al. "Deep learning-based computer-aided diagnosis model for skin cancer detection and classification." *Distributed and Parallel Databases* 40.4 (2022): 717-736.
- [7] Liu, Yu Han. "Feature extraction and image recognition with convolutional neural networks." *Journal of Physics: Conference Series*. Vol. 1087. No. 6. IOP Publishing, 2018.
- [8] Wu, Jiangpeng, et al. "Rapid and accurate identification of COVID-19 infection through machine learning based on clinically available blood test results." *MedRxiv* (2020).
- [9] Ragab, Mahmoud, et al. "Early and accurate melanoma skin cancer detection using the hybrid level set approach." *Frontiers in Physiology* 13 (2022): 2536.
- [10] Melbin, K., and Y. Jacob Vetha Raj. "An enhanced model for skin disease detection using dragonfly optimization based deep neural network." *2019 Third International Conference on I-SMAC (IoT in Social, Mobile, Analytics and Cloud)(I-SMAC)*. IEEE, 2019.
- [11] Verma, Anurag Kumar, and Saurabh Pal. "Prediction of skin disease with three different feature selection techniques using stacking ensemble method." *Applied biochemistry and biotechnology* 191.2 (2020): 637-656.
- [12] Khan, M. Attique, et al. "An integrated skin lesion detection and recognition framework through saliency method and optimal deep neural network features selection." *Neural Computing and Applications* 32.20 (2020): 15929-15948.
- [13] Srinivasu, Parvathaneni Naga, et al. "Classification of skin disease using deep learning neural networks with MobileNet V2 and LSTM." *Sensors* 21.8 (2021): 2852.
- [14] Goceri, Evgin. "Diagnosis of skin diseases in deep learning and mobile technology." *Computers in Biology and Medicine* 134 (2021): 104458.
- [15] Xiong, Xin, XuexunGuo, and Yiping Wang. "Modeling of Human Skin by the Use of Deep Learning." *Complexity* 2021 (2021).
- [16] Khan, Muhammad Attique, et al. "Skin lesion segmentation and multiclass classification using deep learning features and improved moth flame optimization." *Diagnostics* 11.5 (2021): 811.
- [17] Lee, Kyungsu, et al. "Multi-Task and Few-Shot Learning-Based Fully Automatic Deep Learning Platform for Mobile Diagnosis of Skin Diseases." *IEEE Journal of Biomedical and Health Informatics* (2022).
- [18] Adla, Devakishan, et al. "Deep learning-based computer-aided diagnosis model for skin cancer detection and classification." *Distributed and Parallel Databases* 40.4 (2022): 717-736.
- [19] Afza, Farhat, et al. "A hierarchical three-step superpixels and deep learning framework for skin lesion classification." *Methods* 202 (2022): 88-102.
- [20] Bissoto, Alceu, et al. "(De) Constructing bias on skin lesion datasets." *Proceedings of the IEEE/CVF Conference on Computer Vision and Pattern Recognition Workshops*. 2019.
- [21] Ancuti, Codruta O., et al. "Color channel compensation (3C): A fundamental preprocessing step for image enhancement." *IEEE Transactions on Image Processing* 29 (2019): 2653-2665.
- [22] Huether, Brian M., Steven C. Gustafson, and Randy P. Broussard. "Wavelet preprocessing for high range resolution radar classification." *IEEE Transactions on Aerospace and Electronic Systems* 37.4 (2001): 1321-1332.
- [23] Ramamoorthy, M., et al. "Earlier Detection of Brain Tumor by Pre-Processing Based on Histogram Equalization with Neural Network." *Healthcare*. Vol. 10.No. 7.MDPI, 2022.
- [24] Huang, Mengxing, Wenjiao Yu, and Donghai Zhu. "An improved image segmentation algorithm based on the Otsu method." *2012 13th ACIS International Conference on Software Engineering, Artificial Intelligence, Networking and Parallel/Distributed Computing*. IEEE, 2012.
- [25] Garg, Meenakshi, and Gaurav Dhiman. "A novel content-based image retrieval approach for classification using GLCM features and texture fused LBP variants." *Neural Computing and Applications* 33.4 (2021): 1311-1328.
- [26] Chen, Xuan, et al. "An improved Wolf pack algorithm for optimization problems: Design and evaluation." *Plos one* 16.8 (2021): e0254239.
- [27] Basha, SH Shabbeer, et al. "Impact of fully connected layers on the performance of convolutional neural networks for image classification." *Neurocomputing* 378 (2020): 112-119.
- [28] Ngugi, Lawrence C., MoatazAbelwahab, and Mohammed Abo-Zahhad. "Recent advances in image processing techniques for automated leaf pest and disease recognition—A



- review." *Information processing in agriculture* 8.1 (2021): 27-51.
- [29] Lorenzo, Daniel, et al. "Prognostic factors and decision tree for long-term survival in metastatic uveal melanoma." *Cancer research and treatment: official journal of Korean Cancer Association* 50.4 (2018): 1130-1139.
- [30] Priya, R. Devi, et al. "Tri-staged feature selection in multi-class heterogeneous datasets using memetic algorithm and cuckoo search optimization." *Expert Systems with Applications* 209 (2022): 118286.
- [31] Refianti, Rina, Achmad Benny Mutiara, and RachmadinnaPoetriPriyandini. "Classification of melanoma skin cancer using convolutional neural network." *International Journal of Advanced Computer Science and Applications* 10.3 (2019).